Cocurrent Stratified Flow of Immiscible Liquids

RON DARBY and W. W. AKERS

Rice University, Houston, Texas

Velocity profile data were taken in both phases of a cocurrent stratified flow system of two immiscible liquids in the turbulent regime. The data were correlated by a method which combined Pai's results for Poiseuille and Couette flows between parallel plates, resulting in values of the drag coefficients for the wall and interface for both phases. These and other dependent parameters were correlated with flow conditions over a range of flow rates for both phases. Correlations of all parameters except the interfacial drag coefficient were found to be symmetrical; that is, a given correlation applied equally well to data from either phase. The interfacial drag coefficient, on the other hand, depended primarily upon the flow intensity of the upper phase, in a manner which was further dependent upon which phase was the faster.

The lack of adequate understanding of the mechanism of the interaction between two flowing phases has been clearly pointed out by Dukler and Wicks (*1*), who have presented an extensive review and survey of the entire field of gas-liquid flow in conduits, complete with an impressive list of well over two hundred literature references, to arrive at the conclusion that more detailed microscopic measurements are needed for an understanding of the momentum loss process.

The work described here was undertaken to enhance the basic understanding of the momentum transport interaction between two immiscible phases. Specifically, two immiscible liquids, kerosene and water, were studied in cocurrent stratified flow in a rectangular channel of large aspect ratio, so that two-dimensional flow was closely approximated. Velocity profiles were measured in both phases with a hot-wire anemometer as a function of the flow rates of both phases. The flow regime was one of low-level turbulence, the Reynolds numbers for the two phases varying from approximately 2,000 to 6,500. The Reynolds number used here is defined as

$$N_{Re} = \frac{h\,\bar{u}\,\rho}{\mu} = \frac{Q}{\nu} \qquad (1)$$

for each phase. The corresponding Reynolds number based upon a hydraulic radius concept would be from two to four times as large as (1), depending upon whether the interface was included as part of the wetted perimeter.

EQUIPMENT

The experimental equipment and procedures are described in detail elsewhere (*2*). The arrangement, shown in Figure 1, consisted of a transparent plastic channel 15 ft. long and 11½ in. × 2½ in. cross section, diverging at each end over a 3-ft. length to an area of 2 ft. × 1 ft. Separate recirculating systems were provided for both phases. The liquids enter the large end section (separated into two compartments by a horizontal spacer plate), make contact as they enter the rectangular channel, and remain in contact until withdrawn at the downstream expanded section. The flow rates in and out of the channel were controlled to maintain the liquid interface at a steady position between the two withdrawal ports. The tanks and channel were constructed entirely of transparent plastic and all piping was PVC. Glass wool filters were installed in the constant-head tanks to remove any solid contaminants. Because of heating by the centrifugal pumps,

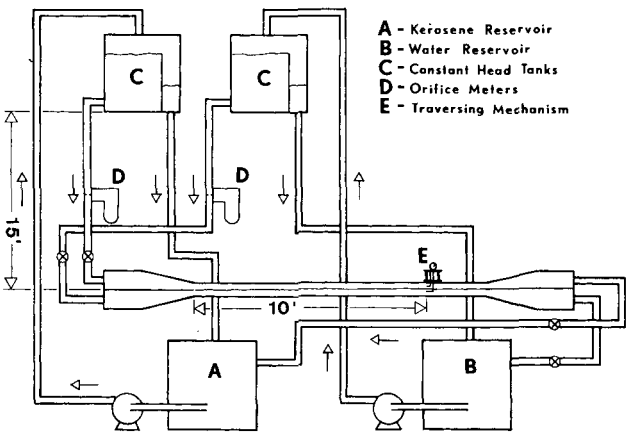

Fig. 1. Schematic of flow system.

both liquids were maintained at approximately 95°F. (to prevent temperature gradients within the system) by means of immersion heaters in the reservoir tanks. About 30 min. of continuous running was necessary to achieve a steady equilibrium temperature. Fluid densities and viscosities were determined from samples withdrawn from the system after several hours of operation. Average density values at the operating temperature were 62.0 and 47.6 lb./cu. ft. for water and kerosene, respectively, and viscosities were 0.734 and 1.22 centipoise, respectively.

Velocities were measured with a two-channel Hubbard Model II HR linear constant temperature hot-wire anemometer. A separate probe was used in each phase to avoid crossing the interface with the hot wire. The probes were constructed to obtain data right up to the interface from both phases; consequently, the regions immediately adjacent to the top and bottom walls could not be reached (10% of the total channel depth). The probes were positioned vertically to within 0.0005 in. by a micrometer screw mechanism located on the channel center line. The probes were calibrated by comparison with observed interfacial velocities; the detailed procedure is described elsewhere (*2*). The anemometer outputs were filtered through a L-R-C filter circuit with a cutoff at about 1 cycle/sec. and then recorded on a Honeywell Visicorder.

DATA

Local mean velocities were measured at a spacing of 0.05 in. in each liquid, reducing to 0.01 near the interface. Approximately thirty to thirty-five readings were made in each phase per run, at least ten being at the closer spacing. Typical profiles are shown in Figure 2, in which velocity and distance

Ron Darby is with Texas A&M University, College Station, Texas.

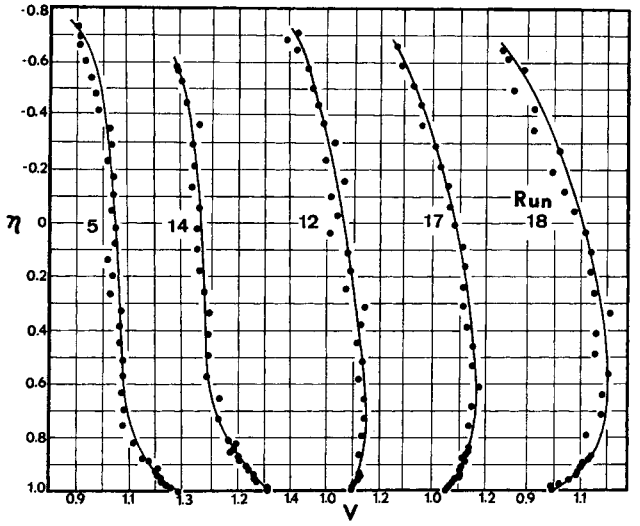

Fig. 2a. Sample velocity profile data, kerosene (upper) phase. Solid lines, Equation (9).

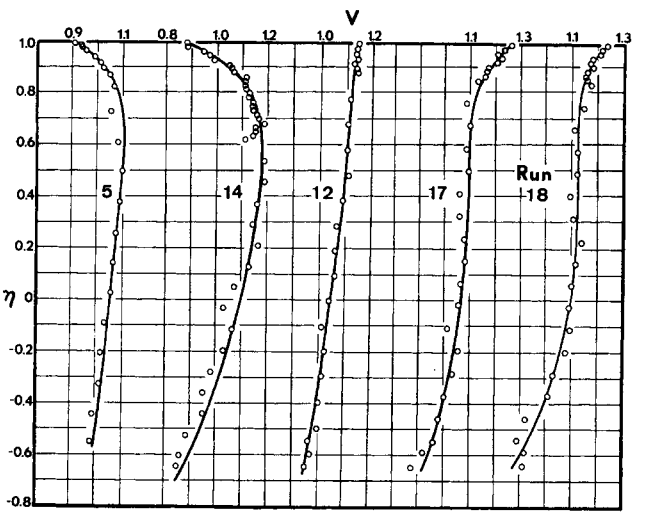

Fig. 2b. Sample velocity profile data, water (lower) phase. Solid lines, Equation (9).

coordinates are made dimensionless by the integrated mean velocity and one-half the phase depth. The origin is at the center of the phase, the positive direction being toward the interface.

Eighteen runs ware made, each at a different combination of flow rates, as indicated in Table 1.

For the flow rates investigated, the interface was essentially flat and planar. The inevitable small amplitude complex disturbance wave structure was present at the interface, although no attempt was made to obtain quantitative measurements of the wave characteristics. Since the region between the crests and troughs of the largest waves could not be explored by the probes, the term *interface* as applied here refers to this finite region rather than to a planar surface. From the difference between the channel depth and the sum of the accessible phase depths, an estimate of the amplitudes of the largest waves in this region is in the range of 0.03 to 0.06 in. for all runs.

THEORY

The usual approach to the analysis of turbulent stratified flow systems is exemplified by the works of Hanratty (3) and of Shearer (4) and Ursell's survey (5), for gas-liquid systems. Attention is focused on one phase (that is, the faster gas phase) to determine the drag effect of the interface. The fluid velocity in this phase is assumed to follow the logarithmic distribution, from which an equivalent interfacial roughness parameter is deduced on the basis of velocity profile or pressure drop data. This approach is fairly successful when applied to systems in which the phase velocities and/or phase depths are of different magnitudes, since the velocity distribution in the slower (more shallow) phase can then be ignored or assumed to be laminar and has a relatively small perturbing effect upon the profile of the faster phase. However for two strata of the same order of velocity and depth, as we have here, the interaction between phases is large as can be seen from the distortion of the profiles in Figure 2, and the logarithmic expression does not adequately describe the data. Further, the logarithmic profile is not adequate in the region near boundaries and interest here centers on the flow profiles of both phases in the vicinity of the interface.

Charles and Lilleleht (6) have correlated pressure drop data for stratified turbulent pipeline flow in terms of the Lockhart and Martinelli (7) parameters with a deviation of 24%. No velocity profile data were included and no detailed analysis was presented.

In view of the shortcomings of previous methods, an alternate approach was attempted which would describe the flow profiles of both phases over the full region of flow.

Consider a separate coordinate system for each phase (Figure 3) with distance measured from the center of the phase toward the interface, and assume the interface

Table 1. Summary of Observed and Calculated Data

Run No.	N_{Re}	m	f_o	f_i	$\overline{u}$, in./sec.	h/D
			Kerosene			
1	2,449	4	0.0142	0.00108	3.74	0.664
2	3,013	5	0.0130	0.00095	4.46	0.686
3	3,487	6	0.0118	0.00123	5.15	0.683
4	3,805	6	0.0105	0.00148	5.66	0.693
5	2,167	4	0.0161	−0.00285	3.30	0.654
6	2,854	5	0.0128	−0.00030	4.40	0.650
7	3,495	5	0.0099	0.00116	5.38	0.656
8	3,798	6	0.0084	0.00118	5.92	0.655
9	2,377	4	0.0131	−0.00228	3.94	0.573
10	2,079	3	0.0133	−0.00352	3.64	0.573
11	2,864	4	0.0102	−0.00057	5.00	0.576
12	3,462	4	0.0094	0.00103	5.95	0.589
13	4,028	5	0.0084	0.00097	6.87	0.598
14	2,164	3	0.0137	−0.00139	4.22	0.512
15	2,721	4	0.0098	−0.00076	5.25	0.529
16	3,568	4	0.0087	0.00105	6.47	0.547
17	3,992	5	0.0081	0.00081	7.36	0.538
18	4,209	5	0.0067	0.00167	7.90	0.532
			Water			
1	2,450	5	0.0151	−0.0059	3.37	0.336
2	2,527	5	0.0157	−0.00086	3.78	0.314
3	2,504	4	0.0153	−0.00091	3.75	0.317
4	2,646	4	0.0145	−0.00031	4.11	0.307
5	3,526	5	0.0113	0.00196	4.71	0.346
6	3,758	5	0.0104	0.00110	4.95	0.350
7	3,561	5	0.0113	−0.00046	4.83	0.340
8	3,574	4	0.0101	−0.00063	4.90	0.345
9	4,274	5	0.0091	0.00152	4.92	0.398
10	5,311	4	0.0066	0.00132	5.76	0.427
11	5,251	4	0.0065	0.00064	5.75	0.424
12	5,069	5	0.0078	−0.00028	5.74	0.411
13	4,917	4	0.0069	−0.00036	5.74	0.402
14	6,766	6	0.0049	0.00137	6.32	0.488
15	6,794	5	0.0058	0.00050	6.76	0.471
16	6,304	5	0.0064	−0.00019	6.32	0.453
17	6,290	4	0.0052	−0.00079	6.19	0.462
18	6,488	4	0.0045	−0.00064	6.38	0.468

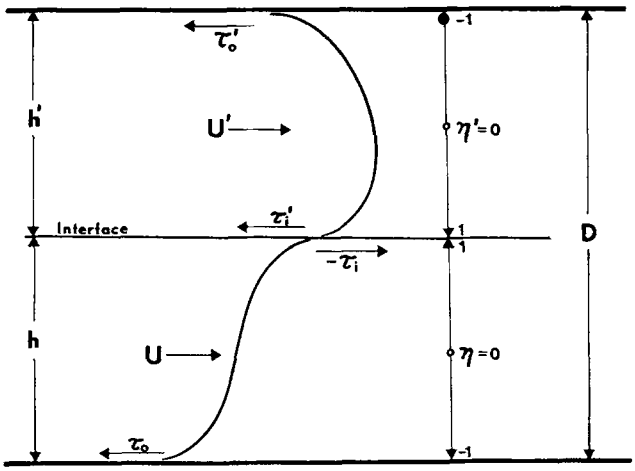

Fig. 3. Stratified cocurrent flow. Coordinate system and sign conventions.

to be a solid boundary moving v
mon to both phases. This presu
a laminar sublayer region in the
a fact which was experimentally
iar method of injecting a dye
within the flowing liquids and i
terface.

By considering only one pha
sign convention on boundary she
3, the turbulent stress within the
olds stress is

$$\tau = \mu \frac{du}{dy} - \rho \overline{u'v'}$$

Since for the above
distributed linearly
the boundaries:

$$\mu \frac{du}{}$$

Integrating (3)
to y and intro
$2\tau/(\rho\bar{u}^2)$, one

$$V = \frac{N_{Re}}{4}\left[(1-\eta^2)\left(\frac{f_o+f_i}{4}\right) + (\eta+1)\left(\frac{f_o-f_i}{2}\right) + \int_{-1} R\, d\eta\right] \quad (4)$$

where $R = \tau/(\frac{1}{2}\,\rho\,\bar{u}^2)$.

Now the proper choice of the dimensionless Reynolds stress R will result in a velocity profile which is valid in the vicinity of the interface. Pai (8) has developed semi-empirical expressions for both Poiseuille and Couette flows between parallel plates which are valid across the entire flow region. These expressions result from an assumed power series for the velocity profile, the initial terms corresponding to laminar profiles with an additional term which is a function of an arbitrary integral exponent and the ratio of turbulent to laminar wall shear. With appropriate values of these two parameters, the expressions can represent velocity profiles from laminar flow through turbulent flow to relatively high Reynolds numbers. [Brodkey (9) has correlated these parameters for Poiseuille Reynolds numbers up to 100,000.]

Now the flow situation in either phase can be considered a combination (or superposition) of Poiseuille flow and Couette flow insofar as the interface corresponds to a rigid boundary moving with velocity u_i. The aforementioned evidence of a laminar boundary-layer region at the interface also supports this premise. Thus for R we shall assume a superposition (that is, a linear combination) of Pai's results for the Reynolds stress from Poiseuille and Couette flows between parallel plates, which are, respectively

$$R_p(\eta) = P\eta\,[1-\eta^{2(n-1)}] \quad (5)$$

$$R_c(\eta) = C\,[1-\eta^{2m}] \quad (6)$$

Here n and m are the integer exponents characterizing Poiseuille and Couette flows, respectively, and P and C are constants (that is, functions of n or m and wall shear, but independent of η).

Inserting $R = R_p(\eta) + R_c(\eta)$ into (4), integrating the following conditions to evaluate P and C

$$V = V_i = u_i/\bar{u} \text{ at } \eta = 1 \quad (7)$$

$$\int_{-1}^{1} V\, d\eta = 2 \quad \text{that is} \quad \int_{-h/2}^{h/2} u\, dy = \bar{u} \quad (8)$$

ve at the following expression for V:

$$= a_o + a_1\eta - a_2\eta^2 - a_3\eta^{2n} + a_4\eta^{2m+1} \quad (9)$$

$$\frac{{}_o + f_i}{} + \frac{3}{}\left(\frac{2n+1}{}\right)(2-V_i) + \frac{2V_i}{N_{Re}}$$

(10)

nts P and C become

$$\frac{f_o+f_i}{4}\Big] \quad (11)$$

$$\left[\frac{4V_i}{N_{Re}} - f_o + f_i\right] \quad (12)$$

ession for the velocity profile, lies to either phase and is a function of the following parameters as applied to that phase: f_o, f_i, N_{Re}, V_i, n, and m. Note that the flow in one phase is not independent of that in the other phase, since any or all of these parameters may be a function of flow conditions in both phases.

Since η is made dimensionless by using the phase depth h, this is an additional parameter which is not independent of flow conditions. This can be seen as follows. By denoting one phase (either) by subscript 1 and the other by subscript 2, a total force balance for a flat horizontal interface gives:

$$-\frac{\Delta P}{\Delta x} = \frac{\tau_{o1}+\tau_{i1}}{h_1} = \frac{\tau_{o2}+\tau_{i2}}{h_2} = \frac{\tau_{o1}+\tau_{o2}}{D} \quad (13)$$

or

$$\frac{h_2}{h_1} = \frac{\tau_{o2}+\tau_{i2}}{\tau_{o1}+\tau_{i1}} = \frac{\rho_2\bar{u}_2^2}{\rho_1\bar{u}_1^2}\left(\frac{f_{o2}+f_{i2}}{f_{o1}+f_{i1}}\right)$$

$$= \left[\frac{\rho_2 Q_2^2}{\rho_1 Q_1^2}\left(\frac{f_{o2}+f_{i2}}{f_{o1}+f_{i1}}\right)\right]^{1/3} \quad (14)$$

Use of a CCD Camera

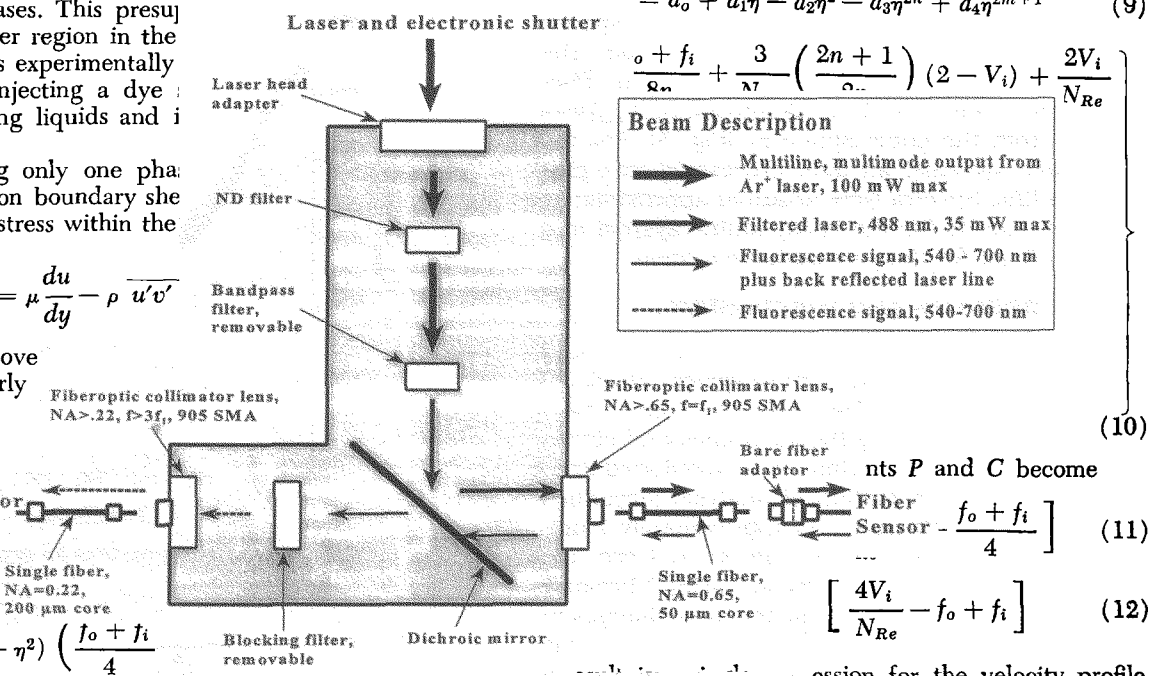

Fig. 3. Diagram of miniaturized and enclosed optical bench.

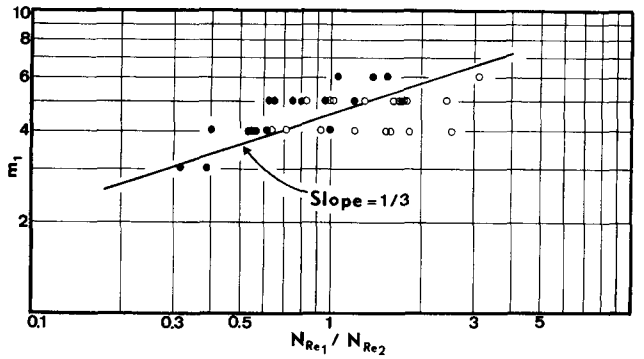

Fig. 4. Exponent in Equation (9) as a function of the ratio of Reynolds numbers. Open circles = water is phase 1; closed circles = kerosene is phase 1.

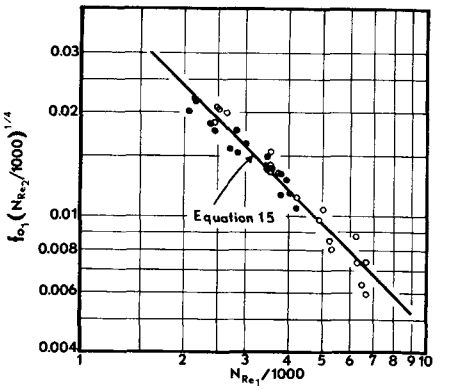

Fig. 5. Correlation of wall drag coefficient. Open circles = water is phase 1; closed circles = kerosene is phase 1.

Also, from (13), $\tau_{i1} = -\tau_{i2}$ (or $\rho_1 \bar{u}_1^2 f_{i2} = -\rho_2 \bar{u}_2^2 f_{i2}$) which is the condition for continuity of shear at the interface, and is hence an implied condition on the force balance, Equation (13).

DISCUSSION

Velocity Profiles

The velocity profile data were used to evaluate f_o and f_i for each run. The data were fit by Equation (9) with a digital computer and a least-mean-square procedure to minimize the sum-of-squares of the deviation with respect to the parameters f_o and f_i. Thus these were calculated directly for assumed values of the integers m and n. The values of m and n were then varied and the procedure repeated until the smallest sum-of-squares of the deviation was found. In practice, the allowed range of m and n was limited to values giving the proper sign for the coefficients in Equation (10) and hence no extraneous inflection points in the curves. The solid lines in Figure 2 represent typical results from this procedure.

The value of n arrived at by this procedure was 5 for all runs for both phases. This value is in general agreement with Brodkey's (9) correlation of Pai's exponent and shear parameters from pipe and channel Poiseuille flow data from various sources. The value of the exponent m varied from 3 to 6, and is tabulated in Table 1 and correlated in Figure 4 as a function of Reynolds numbers for both phases. Since only integral values were used for m, the scatter appears considerable. However a regression analysis of these data reveals a definite correlation, with the exponential valve of 1/3 falling within the 95% confidence limits. Because of the very limited range of this parameter, however, no appreciable significance could be attached to this value.

Wall Shear

The wall friction factor or drag coefficient f_o determined from the profile data is shown in Figure 5. Data from both phases are included, and the solid line is the equation:

$$f_{o1} = 0.047\left(\frac{1{,}000}{N_{Re2}}\right)^{1/4}\left(\frac{1{,}000}{N_{Re1}}\right) \qquad (15)$$

It is emphasized that data for both phases are represented by Equation (15), so that it applies equally to either wall (with the appropriate Reynolds numbers). The form of (15) suggests a combination of the laminar and turbulent (Blasius) friction factors for smooth walls, but further speculations do not appear to be justified at this time.

Interfacial Velocity

The velocity of the interface u_i appears as a parameter in Equation (9) and must be determined as a function of flow conditions. It was found that u_i was 10% greater than the root-mean-square value of the mean velocities of the two phases. If the mean velocities are weighted by the factor μ/h, the interfacial velocity can be represented by the equation

$$\frac{u_i}{\frac{1}{4}(D/\mu_1 + D/\mu_2)} = \frac{1}{\sqrt{2}}\left[\left(\frac{\mu_1 \bar{u}_1}{h_1}\right)^2 + \left(\frac{\mu_2 \bar{u}_2}{h_2}\right)^2\right]^{1/2} \qquad (16)$$

which is the solid line in Figure 6.

Interfacial Position

A comparison of measured values of h_1/h_2 with values calculated from Equation (14) is shown in Figure 7. The depth of each phase h includes one half of the interfacial region, as indicated previously. A considerable portion of the scatter in Figure 7 can be attributed to the uncertainty in determining the actual interfacial position due to the interfacial disturbances. By taking this uncertainty to be the order of the wave amplitude, the resulting uncertainty in h_1/h_2 would be about 8%.

Interfacial Shear

The interfacial friction or drag coefficient f_i was determined from the profile data of each phase for every run. The value of interfacial shear for a given run calculated from the value of f_i for one phase was generally somewhat different from the value calculated from the f_i of the other phase. This is understandable for two reasons. First, the interface is actually a finite region rather than a flat

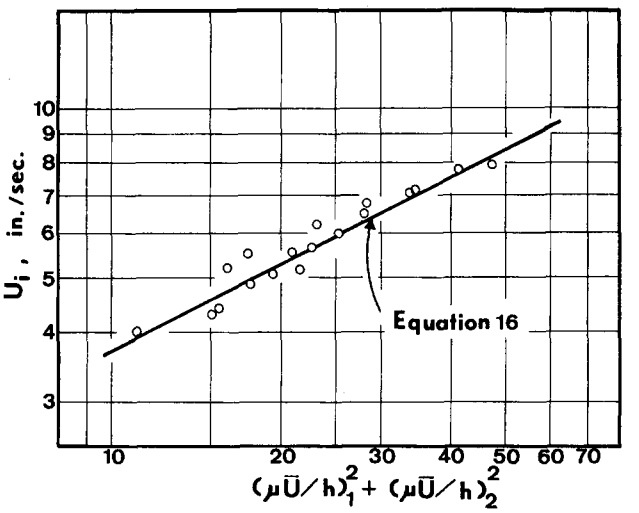

Fig. 6. Correlation of interfacial velocity.

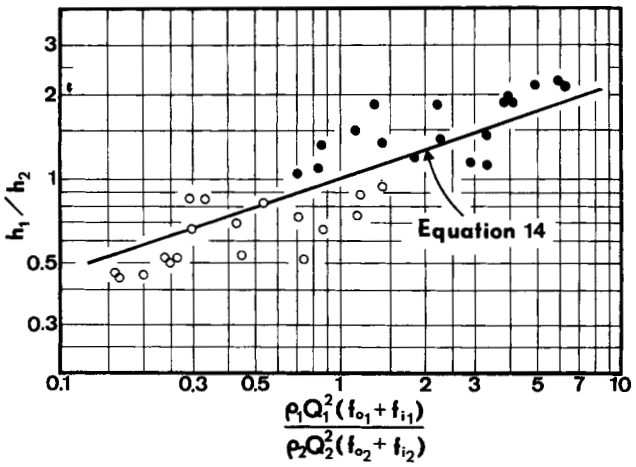

Fig. 7. Correlation of the ratio of phase depths. Open circles = water is phase 1; closed circles = kerosene is phase 1.

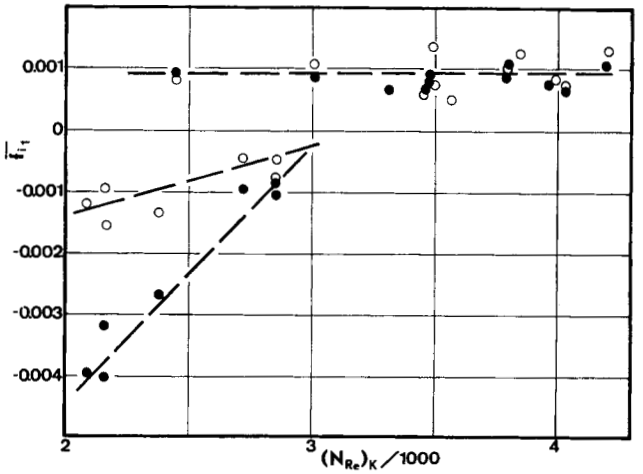

Fig. 8. Mean interfacial drag coefficient as a function of upper (kerosene) phase Reynolds number. Open circles = water is phase 1; closed circles = kerosene is phase 1.

plane, and a shear gradient will exist across such a region. Second, a certain amount of momentum is associated with the waves or disturbances in this region, which is constantly being dissipated by the action of viscosity. To sustain these interfacial waves against dissipation, they must be continuously supplied with momentum at a rate given by the difference in shear forces across the wave region. Similar reasoning has been employed by Stewart (*10*) in considering the generation of water waves by wind, and also by Keulegan (*11*) in considering the stability of stratified miscible liquids and the associated interfacial drag. The relative magnitudes of the interfacial shear values determined here are consistent with this wave momentum mechanism, in that the larger value always occurred on the side of the faster moving phase, which acts as a source for momentum transfer and should thus exhibit the greater boundary shear at the interface. Hence a net flux of momentum should occur from the faster phase into the interfacial or wave region.

Unfortunately, the magnitudes of the shear differences across the interfacial region were too small to provide a reliable correlation. The interfacial shear values were an order of magnitude smaller than the wall shear values, and the variation of interfacial shear across the interfacial region was smaller yet. Therefore an average drag coefficient $\overline{f_i}$ for each phase was used to characterize the interfacial shear. This is defined as

$$\overline{f_{i1}} = \frac{|\frac{1}{2}\,\rho_1\,\overline{u}_1^2\,f_{i1}| + |\frac{1}{2}\,\rho_2\,\overline{u}_2^2\,f_{i2}|}{(\rho\,\overline{u}^2)_1} \qquad (17)$$

The interfacial drag characteristics should logically depend upon the wave or disturbance character of the interface, which in turn should depend upon such parameters as the flow intensities of both phases, relative flow rates, gravity, surface tension contact angle, phase depth, etc. Since only one pair of fluids was studied, with flow rate the only variable, a general correlation cannot be made. The best correlation is shown in Figure 8. In this figure $\overline{f_{i1}}$ is positive when phase 1 is the faster phase, and negative when it is the slower. A similar correlation with the lower fluid (water) Reynolds number was not successful. From this it can be tentatively deduced that the interfacial shear characteristic is primarily a function of the flow intensity of the upper fluid and not of the lower over the range investigated. Furthermore, the interfacial drag coefficient with respect to phase 1 (either phase) appears to be independent of the upper fluid flow intensity when phase 1 is the faster phase, but is strongly influenced by the flow in the upper fluid when phase 1 is the slower phase.

CONCLUSIONS

Velocity profile data for both phases in a cocurrent stratified system in low intensity turbulent flow have been successfully correlated by a method employing a combination of Pai's results for Poiseuille and Couette flow between parallel plates. The method yields values for both wall and interfacial drag coefficients which correlate with flow properties of the two phases. All dependent parameters except the interfacial drag coefficient resulted in symmetrical correlations, that is, a given correlation applied equally well to either phase. The interfacial drag coefficient was found to depend primarily upon the flow intensity of the upper phase and upon which phase is moving the faster. A more general correlation would require a quantitative measurement of the interfacial wave structure as a function of fluid properties and equipment scale as well as flow conditions.

NOTATION

a_o, a_1, a_2, a_3, a_4 = coefficients in Equation (9)
C = coefficient in Equation (6), dimensionless
D = depth of channel, ft.
f = drag coefficient, $2\tau/\rho\overline{u}^2$, dimensionless
h = phase depth, ft.
m = integer exponent in Equation (6), dimensionless
n = integer exponent in Equation (5), dimensionless
N_{Re} = Reynolds number, defined by Equation (1), dimensionless
P = coefficient in Equation (5), dimensionless
Q = volumetric flow rate per unit width, sq.ft./sec.
r = Reynolds stress, lb./sq.ft.
R = dimensionless Reynolds stress, $r/(\frac{1}{2}\,\rho\overline{u}^2)$
u = time-averaged point velocity, ft./sec.
$\overline{u}$ = integrated mean velocity, ft./sec.
u_i = interfacial velocity, ft./sec.
V = dimensionless velocity, $u/\overline{u}$
y = vertical coordinate, ft.

Greek Letters

η = dimensionless vertical coordinate, $2y/h$
μ = viscosity, lb./(sq.ft.)(sec.)
ν = kinematic viscosity, μ/ρ, sq.ft./sec.
ρ = density, lb./cu.ft.
τ = shear stress, lb./sq.ft.

Subscripts

1 = phase one (either)
2 = phase two (either)
i = interface
o = wall

LITERATURE CITED

1. Dukler, A. E., and Moye Wicks III, in "Modern Chemical Engineering," Andreas Acrivos, ed., Vol. I, Reinhold, New York (1963).
2. Darby, Ron, Ph.D. dissertation, Rice Univ., Houston, Tex. (1961).
3. Hanratty, T. J., and J. M. Engen, *A.I.Ch.E. J.*, **3**, 299 (1957).
4. Shearer, C. J., and R. M. Nedderman, *Chem. Eng. Sci.*, **20**, 671 (1965).
5. Ursell, F., in "Surveys in Mechanics," G. K. Batchelor and R. M. Davies, eds., Cambridge (1956).
6. Charles, M. E., and L. U. Lilleleht, *Can. J. Chem. Eng.*, **44**, 47 (1966).
7. Lockhart, R. W., and R. C. Martinelli, *Chem. Eng. Progr.*, **45**, 39 (1949).
8. Pai, S. I., *J. Appl. Mech.*, **20**, 109 (1953).
9. Brodkey, R. S., *A.I.Ch.E. J.*, **9**, 448 (1963).
10. Stewart, R. W., *J. Fluid Mech.*, **10**, 189 (1961)
11. Keulegan, G. H., *J. Res. Natl. Bureau Standards*, **43**, 487 (1949).

Manuscript received December 15, 1965; revision received April 4, 1966; paper accepted April 5, 1966.

A Method of Getting Approximate Solutions to the Orr-Sommerfeld Equation for Flow on a Vertical Wall

BYRON E. ANSHUS and SIMON L. GOREN

University of California, Berkeley, California

A method is presented for getting approximate solutions to the Orr-Sommerfeld equation for free surface flows. The method consists of replacing the velocity, normally a function of distance from the wall, by its value at the free surface while the second derivative of the velocity is kept at its true value. This permits a simple solution to the equation and the eigenvalues can then be determined by a simple and rapid numerical technique. Comparison of this approximate solution for the flow of a thin film on a vertical wall with existing exact numerical solutions and with analytical results valid only for small Reynolds numbers shows the approximation to be quite accurate for most practical values of the parameters and suggests that the method will be useful in investigating the stability of related flows.

A major difficulty in the theory of hydrodynamic stability is the obtaining of accurate solutions to the Orr-Sommerfeld differential equation. In the course of an investigation of finite amplitude wavy flow of a thin film down a vertical wall, we were faced with the problem of finding reasonably accurate solutions to this equation but with a minimum amount of computation. The analytical treatments of Yih (*16, 17*) and of Benjamin (*2*) for infinitesimal disturbances have done much to improve our understanding of the instability of this flow, but their results are limited to flows of low Reynolds number or very low wave number and therefore are not of great practical interest. The numerical techniques of Whitaker (*14, 15*), of Sternling and Barr-David (*10*), and of Sternling and Towell (*11*), while permitting extension of the results to higher Reynolds numbers, are both tedious and time-consuming. In this paper we shall describe a method of getting approximate solutions to the Orr-Sommerfeld equation which seems to be reasonable a priori and which proved to be accurate a posteriori. No attempt is made here to put the approximation on a formal basis or to compute the second term in the approximation; rather, it is our intention to indicate an approximation which is physically reasonable, is easy to carry out, and which proves to be accurate for the present flow. The method should be useful in the investigation of the stability of other flows with a free interface, particularly the flow down a wall of thin films under the influence of surface-active agents.

REVIEW OF PAST WORK

The basic flow whose stability is to be investigated is the parallel flow of a thin film of a Newtonian liquid with constant physical properties under the action of gravity down a flat plate, the film being bounded on the one side by the solid plate and on the other by a free surface subject to capillary forces. By neglecting the air, one finds that the basic velocity profile is a parabola with its vertex at the free surface. Since an excellent review of the literature of film flow, together with a discussion of its practical importance, has been given by Fulford (*4*), we shall review here only the work most pertinent to the present study. Experiments show that this flow is hydrodynamically unstable and that at even small Reynolds numbers the free surface is not smooth but rippled.

Yih (*16*) was the first to attack the problem of the stability of this flow along the lines of classical (linearized) hydrodynamic stability theory. In this treatment (*9*) infinitely small velocity disturbances with a stream function of the form $\phi(y)e^{i\alpha(x-ct)}$ are assumed to be superimposed on the mean parabolic flow. $c = c_R + ic_I$ is the complex wave velocity and is found as an eigenvalue of the problem as a function of the wave number α, the